A Circularly Polarized 60 GHz Microstrip Antenna

Here is a mm-wave antenna suitable for WLAN systems

By V. A. Volkov, M. D. Parnes
Ascor, and
V. D. Korolkov and R. G. Shifman
Resonance

This article presents the design of a microstrip radiator-based circularly polarized antenna for the operation range of 59 to 61 GHz. Characteristics of the antenna are appended. This antenna, owing to its inherent simplicity, cheapness and small size, can be used in transceivers for 60 GHz wireless local networks.

High-speed and high-capacity in-office wireless local networks have recently become in large demand. In addition, since the centimeter waves' range has been congested, international recommendations appeared to bring some of the millimeter wavelength subranges to commercial employment.

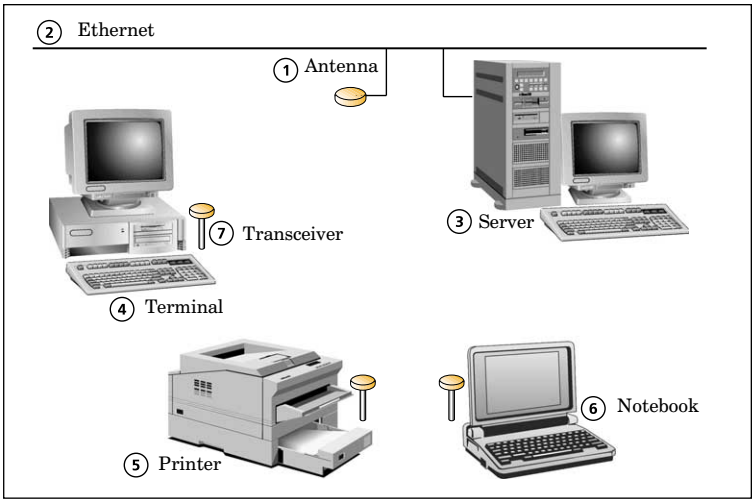

▲ **Figure 1. A 60 GHz wireless local network.**

Figure 1 shows the 60 GHz wireless local network that is intended for indoor use, allowing data transfer at the rate of 10 Mbit/s. Two microstrip antennas (receiving and transmitting) are connected to a high frequency module. Microstrip antennas are built from a number of standard units, at the user station and from a single unit, in the operation sites distributor. They radiate and receive circularly polarized waves to minimize the influence of multiple reflections in the room. In the operation sites distributor, the antenna beamwidth from 60 to 80 degrees would suffice to cover a rather large territory.

This article discusses the design sequence of a single-unit circularly polarized 60 GHz microstrip antenna. A circularly polarized electromagnetic wave can be obtained using two mutually perpendicular, equi-amplitude, linearly polarized waves that are in phase quadrature relative to each other. Then, if a microstrip patch (MSP— a square-shaped microstrip radiator) is excited on two sides by equi-amplitude oscillations with the phase difference of 90 degrees between them, the total field radiated by all MSPs will be circularly polarized.

The idea of circular polarization resulting from the excitation of two spatially orthogonal modes in the antenna is the basis for all rotary polarization MSPs. Various approaches can make the idea a reality. Presented here is the simplest technique: a quadrature hybrid is used to divide the power into two equi-amplitude parts in phase quadrature.

Calculation and design

Figure 2 illustrates the antenna design and method of mating with the UG-358/U standard

waveguide flange. A board (1) (h = 0.25 mm in thickness), including both the radiator and the bridge, together with the 0.25 mm-thick dielectric layer (2) and the upper screen (3), form a balanced stripline with b = 0.5 mm. The antenna pedestal is designed as a special configuration waveguide flange (4) with a 0.5 mm deep slot to receive both the strip circuit and the waveguide-to-stripline adapter. A quarter-wavelength waveguide short (5) provides the optimal connection between the balanced stripline and the standard-size waveguide (3.8 × 1.9 mm).

The strip board incorporates the microstrip patch (radiator) and the quadrature hybrid. In this case, the radiator and the matching quarter-wave transformer are constructed on an unbalanced microstrip line, while the hybrid, the pill and the waveguide-to-strip adapter are based on a balanced stripline. The Rogers Corp. cladded sheet dielectric (R3003, h = 0.25 mm, ε = 3.02 ± 0.1) was selected as material for the antenna. First, both the geometry and the frequency response of the microstrip part of antenna were defined. Then the MSP with the quadrature hybrid and calculation of polarization characteristics of the antenna was integrated.

Figure 3 depicts the antenna configuration and the six-pole equivalent circuit where 1 and 1' are the input terminals and 2 and 2' and 3 and 3' are outputs of high-resistance probes. The electric models do not take into account physical dimensions of the probes considering them as lumped elements. With the supposition of negligible spacing between exciting points compared to the free-space wavelength, it is obvious that complex amplitudes of the resulting spatially-orthogonal electric field components E_x and E_y vary in proportion with the transmission gains s_{12} and s_{13}, respectively. That is, $E_x \sim s_{12}$ and $E_y \sim s_{13}$ or $P_x \sim |s_{12}|2$ and $P_y \sim |s_{13}|2$, where P_x and P_y are the averaged densities of the power fluxes transferred by the orthogonal components E_x and E_y, respectively).

Accordingly, estimation of MSP polarization properties is reduced to calculation of the full multiport scattering matrix, using the microwave device analysis program similar to that described in [1]. The program permits calculation of the full multiport scattering matrix from known s-matrices of its components. Whereas the program leaves room only for editing to allow new element definition subprograms to be entered. We have corrected the available description of the element "the open end of microstrip line," i.e. MSP, according to the terminology adopted in the paper.

It is known that MSP can be modeled by the equivalent circuit in the form of a transmission line section with the length that differs from the actual length L by the value Δl, which is the MSP extension on both ends, due to the edge capacitances (such as with allowance made for existence of the edge fields). The transmission line is loaded by the real resistance R_r that is equivalent

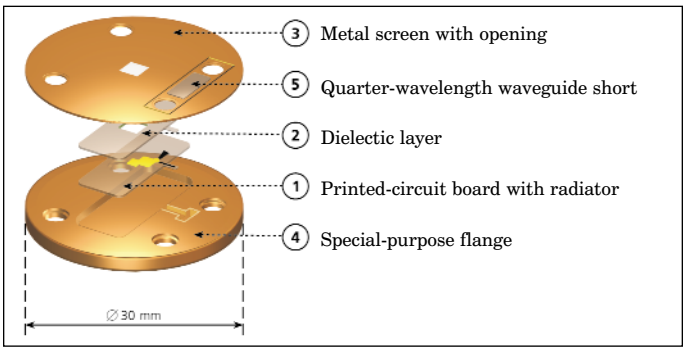

▲ **Figure 2. Configuration of the antenna.**

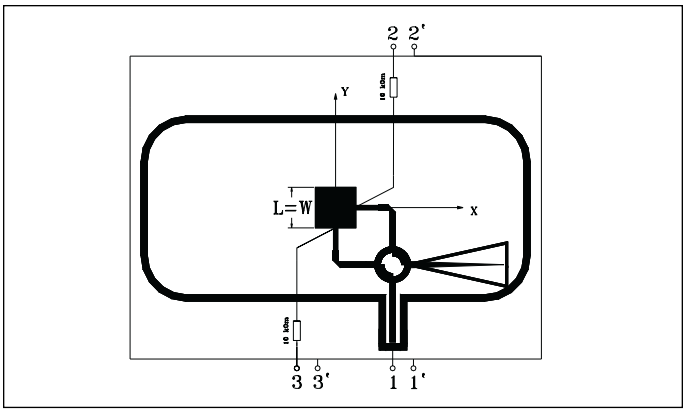

▲ **Figure 3. Printed-circuit board topology.**

to the ohmic loss by energy radiation.

The dispersion influence on the quasi-static expansion Δl_{st} value was studied in [2], where the authors have shown that, for the millimeter range of wavelengths, the dispersion expansion Δl_f appears to be substantially shorter than the Δl_{st} value obtainable using a quasi-static approximation.

As shown in [3] and [4], the frequency depended wave impedance Z_0 (f) and the effective dielectric constant vs. frequency ε_{re} (f) can be represented as follows:

$$Z_0(f) = Z_{0t} - \frac{Z_{0t} - Z_0}{1 + G\left(\frac{f}{f_p}\right)^2} \quad (1)$$

$$\varepsilon_{re}(f) = \varepsilon_r - \frac{\varepsilon_r - \varepsilon_{re}}{1 + G\left(\frac{f}{f_p}\right)} \quad (2)$$

where

$$G = \left(\frac{Z_0 - 5}{60}\right)^{0.5} + 0.004Z_0 \quad (3)$$

$$f_p = \frac{0.3976 Z_0}{h} \tag{4}$$

In these equations, f_p is measured in GHz, h is measured in millimeters, and Z_0 and Z_{0t} are measured in ohms. Z_0 and Z_{0t} are the wave impedance of the stripline of width (w), height (h and $2h$), respectively. ε_{er} is the effective dielectric constant. Both Z_0 and ε_{er} are the known quasi-static values [1].

In the final analysis, the input reflectivity of the $L + \Delta l\ (f)$ long regular line, when loaded by the real resistance R_r, was computed from the known formula with regard to imaginary inhomogenities and to the effect of dispersion. A novel expression has been obtained for R_r from numerous experimental observations:

$$s_{11} = \frac{1 - j \cdot tg\left[\beta(L + \Delta 1_f)\right]}{1 + j \cdot tg\left[\beta\left(L + \Delta 1_f\right)\right]}\left(\frac{R_r - 1}{R_r - 1}\right) \tag{5}$$

where

$$\beta = \left(\frac{2\pi}{\lambda_0}\right)\sqrt{\varepsilon_{re}(f)} \tag{6}$$

$$R_r = \left(\frac{1}{Z_0(f)}\right)\left(\frac{60\lambda_0^2}{\omega^2} + \frac{90}{e^{8\pi\left(1-\frac{\omega}{\lambda 0}\right)} + 1}\right), \text{ for } \omega < 0.35\lambda_0 \tag{7}$$

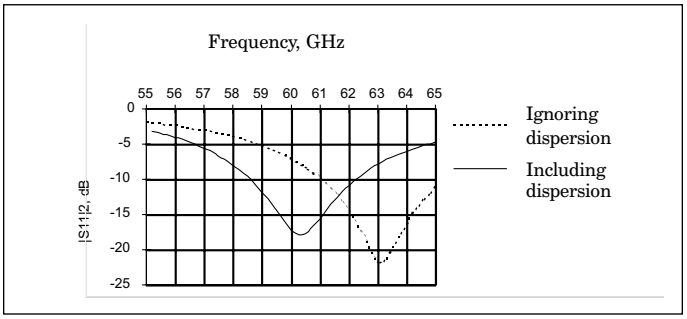

▲ **Figure 4. Theoretical return loss for the microstrip patch, 1.2 × 1.28 mm in size, with the matching quarter-wave transformer.**

$$\frac{\Delta l_f}{h} = 0.412\left(\frac{\varepsilon_{re}(f) + 0.3}{\varepsilon_{re}(f) - 0.258}\right)\left(\frac{\omega + 0.264h}{\omega + 0.8h}\right) \tag{8}$$

Figure 4 gives estimated frequency dependencies of $|s_{11}|^2$ for the microstrip patch, 1.28 × 1.28 mm in size, with the matching quarter-wave transformer, either with or without regard to dispersion effects.

There are two typical design alternatives for the quadrature hybrid. One topology provides a matched load available in the fourth isolated arm; the other has no load in the fourth arm.

Figures 5 and 6 present both the gain-frequency and the phase-frequency characteristics of the equivalent six-pole circuit transfer coefficients s_{12} and s_{13} for both alternative quadrature hybrid designs.

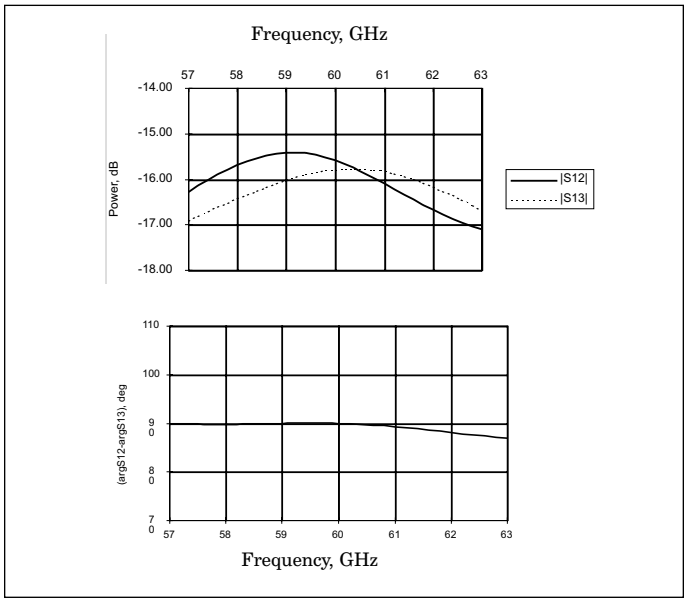

▲ **Figure 5. The transfer coefficient gain- frequency (a) and phase frequency (b) characteristics of the equivalent six-pole circuit incorporating a matched load quadrature hybrid.**

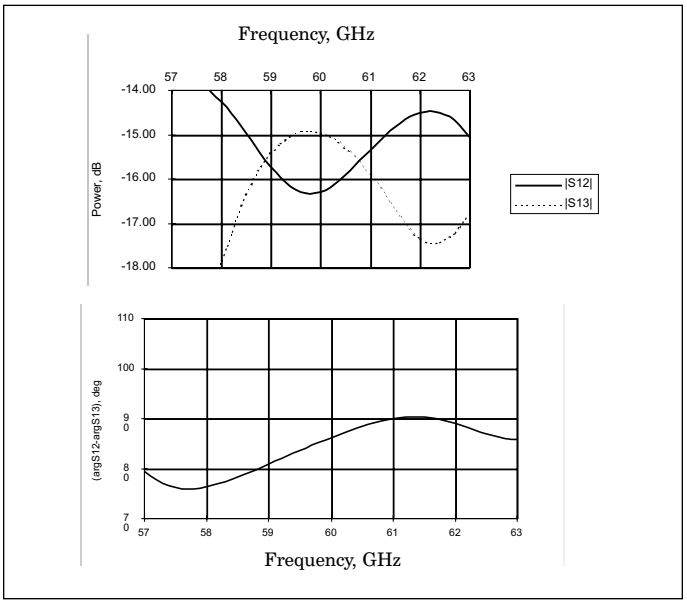

▲ **Figure 6. The transfer coefficient gain-frequency (a) and phase-frequency of the equivalent six-pole circuit incorporating a quadrature hybrid with no load.**

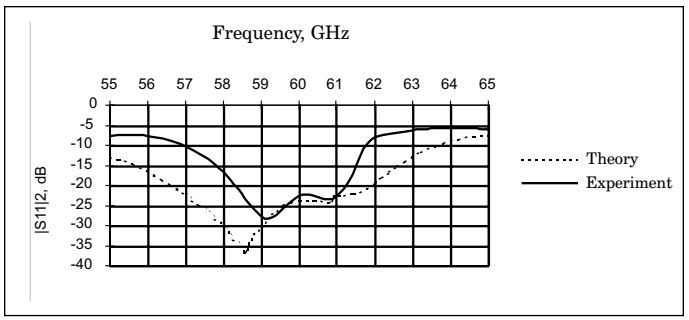

▲ **Figure 7. Antenna's return loss vs. frequency.**

The vital distinction between the show loaded circuit frequency response and that of the unloaded circuit provide clear evidence in support of the rather apparent but sometimes forgotten statement that any unreasonable idealization of the device to be developed is inadmissible at the simulation stage.

Experimental results

The topology version presented in Figure 3 was accepted for implementation as the best suitable to fit requirements of circular polarization. It was supposed to use a dielectric wedge made of 16 m thick tantalum film as a matched load in the bridge circuit.

Shown in Figure 7 is the MSP frequency characteristic that was measured with the following waveguide-to-strip adapter parameters: depth of the strip immersion in the waveguide –0.62*b* and the short circuit plane is to be offset by 0.21 λ_0 from the strip, where *b* is the width of the narrow waveguide wall and λ_0 is the waveguide wavelength that corresponds to the central frequency of the given range (60 GHz).

Polarization characteristics were measured using a horn rotating around the longitudinal axis. The measuring error due to the cross-polarization loss was about 20 dB. The peak power response $W_{||}$ was observed under such conditions when the horn plane *E* was parallel to the major axis of the polarization ellipse and the minimum response $W_{\perp}$, when *E* was perpendicular to that axis. Just as the amplitude ratio = E_{0x}/E_{0y}, so the phase difference δ between E_x and E_y were determined from the experimentally found values of $W_{||}$, W⊥ and τ (the polarization inclination) using the relationships [5] that correlate two forms of the polarization ellipse description (canonic and parametric). It follows then that a polarization ellipse can be represented parametrically using the field components and basing on the measured values, as in the calculation:

$$E_x = E_{0x}\sin(\omega t) \tag{9}$$

$$E_y = E_{0y}\sin(\omega t + 8) \tag{10}$$

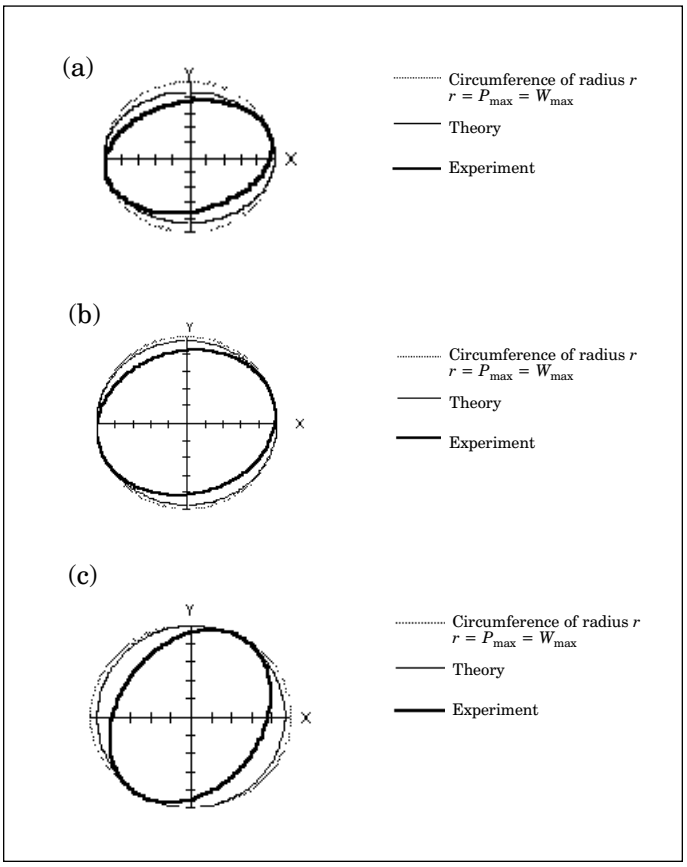

▲ **Figure 8. Polarization ellipses for MSP waves radiated with frequencies (a) 59.0 GHz, (b) 60.0 GHz and (c) 61.0 GHz.**

Parameters of Polarization	Frequency, GHz		
	59	60	61
q^2, dB	1.4	0.8	-1.4
τ, degreed		15	15 50
p_c	0.986	0.996	0.986

▲ **Table 1. Polarization ellipse parameters measured at the frequencies of 59, 60 or 61 GHz.**

where E_{0x} and E_{0y} are amplitudes of orthogonal electric field components.

Figure 8 shows both theoretical and experimental polarization ellipses for MSP radiated waves such as 59, 60 and 61 GHz. Table 1 gives polarization ellipse parameters, such as the axial ratio *q*, the inclination τ and the circular polarization efficiency p_c, that were measured with the frequency of 59, 60 or 61 GHz. The circular polarization efficiency was determined from the expression:

$$P_c = \sqrt{1 - \left(\frac{W_{11} - W_1}{W_{11} + W_1}\right)^2} \qquad (11)$$

The microstrip antenna pattern is shown in Figure 9.

Conclusion

The proposed microstrip antenna provides the required beam width and circular polarization parameters at the frequency 60 GHz. The stripline antenna design, including a waveguide input, promises high manufacturability and low cost in mass production.

The analytic relationships used for computing real and imaginary components of the MSP input impedance have been effective in estimation, with a high degree of precision (> 2 percent), both of the radiator resonant frequency and of the radiator-to-free space matching frequency band, allowing to avoid an extra iteration in designing printed antenna topology.

This article has demonstrated essential differences in directional coupler frequency characteristics between real devices with a matched load available in the isolated arm and those with the missing fourth arm. It is hoped that this finding will serve as a reminder of the typical designer's delusion — a priori abstraction of the device that is to be developed. ■

References

1. K. C. Gupta, R. Garg, R. Chadha, *Computer-Aided Design of Microwave Circuit,* Artech House, 1981.

2. T. Itoh, "Analysis of Microstrip Resonators," *IEEE Trans. Microwave Theory Tech.*, Vol. MTT-22, November 1974.

3. B. Branco, et al., "Frequency Dependence of Microstrip Parameters," *Alta Frequenza*, Vol. 43, 1974.

4. T. C. Edwards and R. P. Owens, "2-18 Ghz Dispersion Measurements on 19-100 Ohm Microstrip Line on Sapphire," *IEEE Trans. Microwave Theory Tech.*, Vol. MTT-24, August 1976.

5. J. D. Kraus, *Radio Astronomy*, McGraw-Hill Book Company, 1967.

Author information

V.A. Volkov and M.D. Parnes are employed with Ascor, and V.D. Korolkov and R.G. Shifman are employed with Resonance; both companies are headquartered in St. Petersburg, Russia. All authors may be reached by phone/fax at + 44 7 812 5538445. Mr. Parnes may be reached via e-mail at ascor@parnes.spb.ru, and Mr. Shifman may be reached at shifman@resonance.spb.ru. Ascor's web address is www.ascor.eltech.ru.